JCI The Journal of Clinical Investigation

A molecular switch controls interspecies prion disease transmission in mice

Christina J. Sigurdson, … , Kurt Wüthrich, Adriano Aguzzi

J Clin Invest. 2010;120(7):2590-2599. https://doi.org/10.1172/JCI42051.

Research Article **Neuroscience**

Transmissible spongiform encephalopathies are lethal neurodegenerative disorders that present with aggregated forms of the cellular prion protein (PrP^C), which are known as PrP^{Sc}. Prions from different species vary considerably in their transmissibility to xenogeneic hosts. The variable transmission barriers depend on sequence differences between incoming PrP^{Sc} and host PrP^C and additionally, on strain-dependent conformational properties of PrP^{Sc}. The β_2-α_2 loop region within PrP^C varies substantially between species, with its structure being influenced by the residue types in the 2 amino acid sequence positions 170 (most commonly S or N) and 174 (N or T). In this study, we inoculated prions from 5 different species into transgenic mice expressing either disordered-loop or rigid-loop PrP^C variants. Similar β_2-α_2 loop structures correlated with efficient transmission, whereas dissimilar loops correlated with strong transmission barriers. We then classified literature data on cross-species transmission according to the 170S/N polymorphism. Transmission barriers were generally low between species with the same amino acid residue in position 170 and high between those with different residues. These findings point to a triggering role of the local β_2-α_2 loop structure for prion transmissibility between different species.

A molecular switch controls interspecies prion disease transmission in mice

Christina J. Sigurdson,[1,2,3] K. Peter R. Nilsson,[3] Simone Hornemann,[4] Giuseppe Manco,[3] Natalia Fernández-Borges,[5] Petra Schwarz,[3] Joaquín Castilla,[5,6] Kurt Wüthrich,[4,7] and Adriano Aguzzi[3]

[1]Department of Pathology and Department of Medicine, University of California, San Diego, La Jolla, California, USA. [2]Department of Pathology, Immunology, and Microbiology, University of California, Davis, Davis, California, USA. [3]UniversitätsSpital Zürich, Institute of Neuropathology, Zürich, Switzerland. [4]Institut für Molekularbiologie und Biophysik, ETH Zürich, Zürich, Switzerland. [5]CIC BioGUNE, Parque tecnológico de Bizkaia, Bizkaia, Spain. [6]Ikerbasque, Basque Foundation for Science, Bizkaia, Spain. [7]Department of Molecular Biology and Skaggs Institute for Chemical Biology, The Scripps Research Institute, La Jolla, California, USA.

Transmissible spongiform encephalopathies are lethal neurodegenerative disorders that present with aggregated forms of the cellular prion protein (PrP^C), which are known as PrP^{Sc}. Prions from different species vary considerably in their transmissibility to xenogeneic hosts. The variable transmission barriers depend on sequence differences between incoming PrP^{Sc} and host PrP^C and additionally, on strain-dependent conformational properties of PrP^{Sc}. The β_2-α_2 loop region within PrP^C varies substantially between species, with its structure being influenced by the residue types in the 2 amino acid sequence positions 170 (most commonly S or N) and 174 (N or T). In this study, we inoculated prions from 5 different species into transgenic mice expressing either disordered-loop or rigid-loop PrP^C variants. Similar β_2-α_2 loop structures correlated with efficient transmission, whereas dissimilar loops correlated with strong transmission barriers. We then classified literature data on cross-species transmission according to the 170S/N polymorphism. Transmission barriers were generally low between species with the same amino acid residue in position 170 and high between those with different residues. These findings point to a triggering role of the local β_2-α_2 loop structure for prion transmissibility between different species.

Introduction

Transmissible spongiform encephalopathies (TSEs) are lethal neurodegenerative disorders that include kuru and Creutzfeldt-Jakob disease (CJD) in humans, bovine spongiform encephalopathy (BSE) in cows, scrapie in sheep and goats, and chronic wasting disease (CWD) in cervids (1). A crucial component of the infectious agent is PrP^{Sc}, a highly aggregated, β-sheet–rich isoform of the cellular prion protein (PrP^C) (2, 3).

Prion diseases can occur as distinct strains within species expressing identical PrP amino acid sequences (4). Prion strains have originally been defined by transmission to mice, in which they show different incubation periods (ips) and variable brain regions targeted (5–7). Evidence is accumulating that distinct strains represent different PrP^{Sc} conformations (8–11).

There is evidence that interspecies prion transmission occurs in nature, and it has thus become an important food safety issue. Dietary exposure to beef contaminated with the BSE agent is believed to have caused nearly 200 cases of variant CJD (vCJD) in humans (12–15) as well as spongiform encephalopathies in domestic cats and British zoo animals (16–19). Prion transmission across species barriers has been replicated experimentally and typically leads to incomplete attack rates and to prolonged, highly variable ips (20). Understanding the factors that dictate species barriers is crucial for assessing the risk for human prion disease, particularly as new prion strains may arise in food animals (21–24).

Experimental studies of species and strain barriers in vitro and in vivo indicate that certain amino acid positions have an outstandingly strong influence on prion transmission among species with heterologous prion protein (*Prnp*) sequences (4, 25–32). For example, hamsters resist infection with mouse prions, although the hamster and mouse *Prnp* sequences differ at only 9 residues (30–32). Similarly, knock-in mice that only differ from WT mice at codon 101 of the *Prnp* allele show highly divergent susceptibility to sheep scrapie, BSE, and CJD (33, 34).

Susceptibility to natural prion infections may also be influenced by *Prnp* polymorphisms. Humans are polymorphic at *PRNP* codon 129 (methionine/valine). While approximately 38% of Europeans are 129MM homozygous, 100% of the confirmed vCJD cases have occurred in 129MM patients (35), indicating selective susceptibility of this allotype to BSE prions. Since the efficiency of TSE transmission into a new species further appears to vary depending on the prion strain (33, 36, 37), the increased susceptibility of humans carrying the 129MM alleles may not be maintained with future BSE strains.

Although the amino acid sequence of PrP^C is overall highly conserved among mammals, the β2-α2 loop encompassing residues 165–175 is a site of outstandingly high sequence diversity (38). The 3-dimensional structure of PrP^C immediately led to the identification of this loop as a key part of the surface epitope that might influence species barriers (39, 40), and this hypothesis also received support from molecular dynamics simulations (41). Mature PrP^C contains a flexibly unstructured N-terminal 100-residue "tail" and a globular C-terminal domain of similar size, which contains 3 α-helices and a short antiparallel β-sheet (40, 42, 43). The β_2-α_2 loop is structurally polymorphic in that amino acid sequences that contain 170S and 174N form a poorly defined loop in the NMR solution structures at 20°C (44–47), whereas sequences that contain 170N, or 170N and 174T (numbering according to ref. 48) have a well-defined loop (49–51). Here, we

Conflict of interest: Adriano Aguzzi receives funding from the Novartis Foundation.
Citation for this article: *J Clin Invest.* 2010;120(7):2590–2599. doi:10.1172/JCI42051.

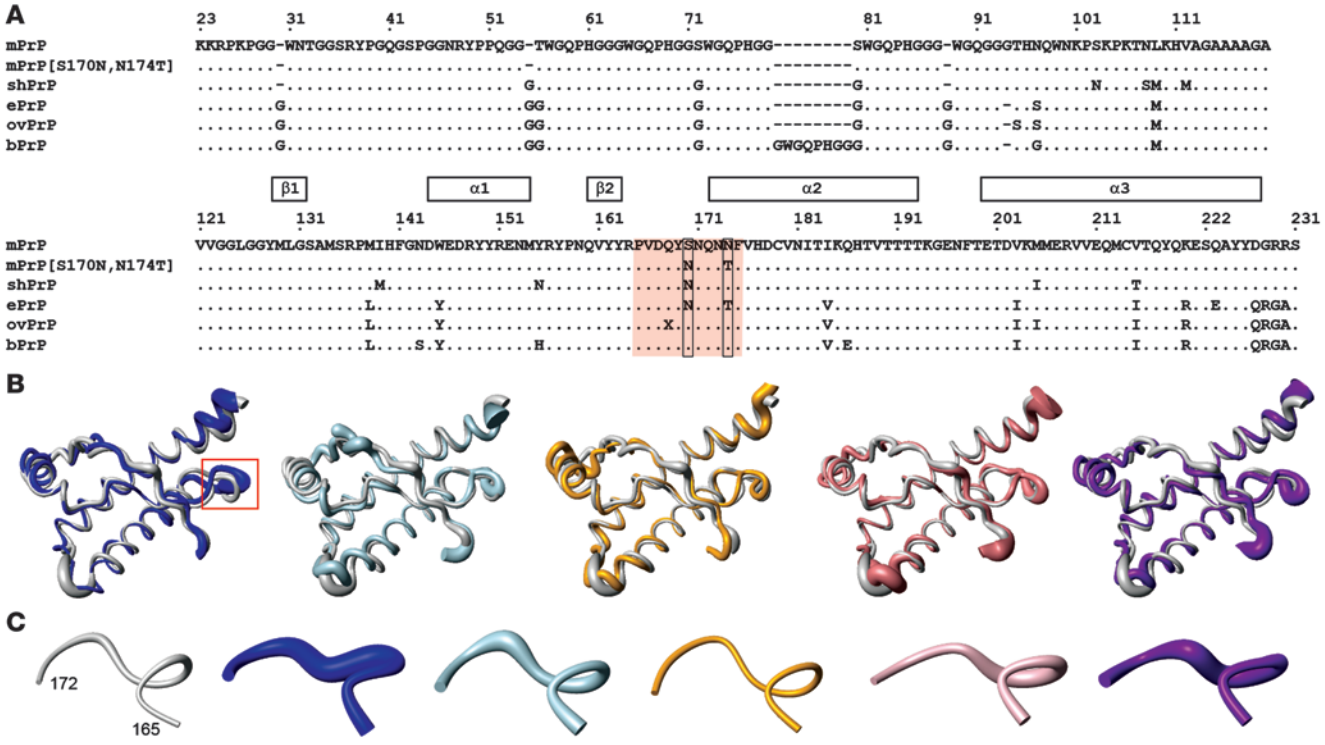

Figure 1
Amino acid sequence and 3-dimensional structure comparisons for WT mouse PrP^C (*Prnp* a), mouse RL-PrP^C, and for WT-PrP^C of 4 additional mammalian species. (**A**) PrP amino acid sequence of PrP from mouse (mPrP; *Mus musculus*, AAA39997) and the RL variant thereof and Syrian hamster (shPrP; *Mesocricetus auratus*, AAA37091), elk (ePrP; *Cervus elaphus nelsoni*, AAB94788), sheep (ovPrP; *Ovis aries*, ABC61639), and cattle PrP (bPrP; *Bos taurus*, ABU97893). For mouse PrP^C, the residues 23–231 are shown. For the RL variant and the other species, the only amino acids indicated are those that differ from the mouse PrP sequence, with identical amino acids indicated by dots and deletions indicated by dashes. The shaded region indicates the β_2-α_2 loop region, and the "X" in the ovine indicates a polymorphic residue position (Q/R). At the top, the regular secondary structure elements are shown. (**B**) Backbone superpositions of residues 125–228 of RL-PrP^C (gray) with mouse PrP^C (dark blue), Syrian hamster PrP^C (light blue), elk PrP^C (yellow), sheep PrP^C (pink), and cattle PrP^C (purple) (adapted from refs. 44–47, 51). A larger view of the region in the red box is shown in **C**. (**C**) Backbone fold of residues 165–172 in RL-PrP^C, mouse PrP^C, Syrian hamster PrP^C, elk PrP^C, sheep PrP^C, and cattle PrP^C. The radius of the cylindrical rods representing the polypeptide chains is proportional to the mean global backbone displacement for residues from 20 conformers used to represent the NMR structures. The same color code is used as in **B**.

used transgenic mice expressing prion proteins that differ in discrete sequence positions of the β_2-α_2 loop to further investigate the effect of the loop structure on interspecies prion transmission. We found that sequence variations affecting only the β_2-α_2 loop conformation can significantly impact cross-species susceptibility to a broad array of prion diseases.

Results

To determine the impact of the loop sequence on interspecies transmission, we used 2 lines of transgenic mice expressing PrP^C variants that differ by 2 amino acid residues. *tga20* mice overexpressed WT mouse PrP, whereas *tg*1020 mice overexpressed a "rigid loop" (RL) variant of PrP with S170N and N174T substitutions (Figure 1A). In both mouse lines, the transgene was expressed in the context of a "half-genomic" prion minigene construct. Expression levels were approximately 6- and 3-fold higher in *tga20* and *tg*1020 mice, respectively, than those for endogenous PrP^C (52, 53).

Mice were inoculated with prions derived from 5 species (Figure 1A), for which PrP^C 3-dimensional structures have been fully characterized by solution NMR spectroscopy: sheep, cattle, cervid, hamster, and mouse (Figure 1B). The overall structure of the C-terminal globular domain is nearly identical among these 5 species (Figure 1B), yet they differ in the local conformations of the β_2-α_2 loop (Figure 1C) encompassing residues 165–175 (40, 44–47, 50, 51).

Inoculation with mouse scrapie strains. All prion strains used for the inoculations were proteinase K (PK) resistant. Therefore, the criterion used for determining transmission to *tg*1020 and *tga20* mice was the presence of PK-resistant PrP^{Sc} in the brain of the recipients as well as development of a rapidly progressive neurologic disease with widespread spongiosis. To assess the susceptibility of WT-PrP and RL-PrP mice to mouse-adapted scrapie, we inoculated *tga20* and *tg*1020 mice intracerebrally with 10^4 LD_{50} of Rocky Mountain Laboratory (scrapie strain passage 5, referred to herein as RML5) prions (Figure 2A). *tga20* mice developed terminal prion disease in 74 ± 6 days, whereas *tg*1020 mice developed disease after a much longer and more variable ip (323 ± 92 days; unpaired, 2-tailed Student's *t* test, $P = 0.002$; Figure 2B and Table 1). The prion-containing brain homogenate recovered from the latter mice was termed $RL\text{-}RML^1$ (RL-passaged RML, first passage). WT mice developed scrapie in 170 ± 12 days after inoculation with 10^3 log LD_{50} of the same inoculum (Figure 2B), indicating that RL-PrP mice developed disease with a 47% increase in the ip compared with the WT mice.

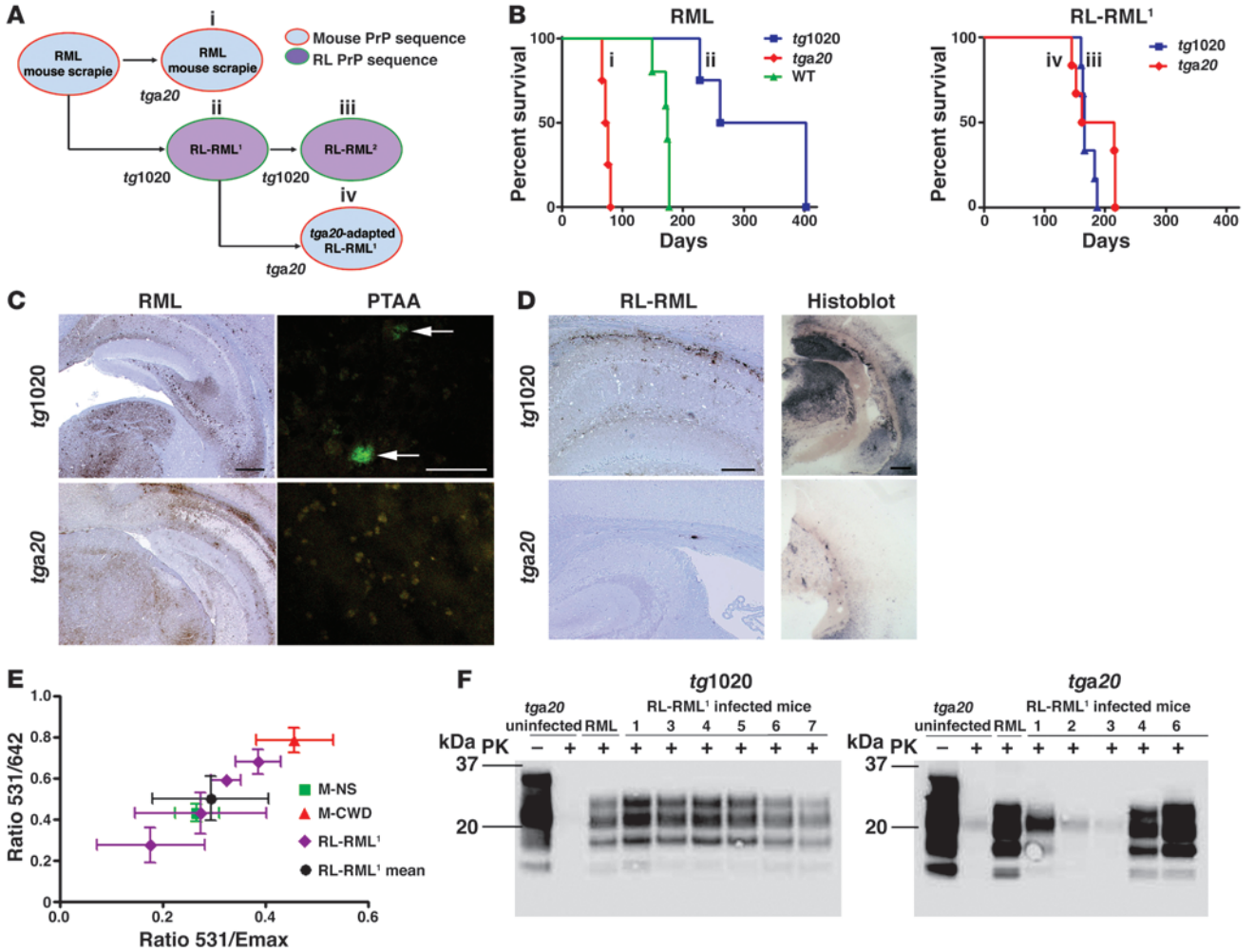

Figure 2

The RL induces a species barrier for RML infection. (**A**) Schematic illustrating the passages of RML mouse-adapted scrapie into the *tga20* and *tg*1020 mice. The labels i–iv indicate the inoculation groups labeled in the survival curves in **B**. (**B**) RML induces prion disease in *tg*1020 mice after a prolonged, highly variable ip (blue line). In contrast, *tga20* mice infected with RML have a short, invariable ip (red line). WT mice infected with RML are shown for comparison. RL-RML^1 leads to a shortened, more consistent ip in *tg*1020 mice but a prolonged, variable ip in *tga20* mice, indicative of a species barrier effect. (**C**) Diffuse PrP^{Sc} staining occurs in the brain after RML infection of *tg*1020 and *tga20* mice. Only aggregates in *tg*1020 mice were positive with PTAA staining (arrows). Scale bars: 400 μm (RML); 50 μm (PTAA). (**D**) Passage of the RL-RML resulted in abundant PrP^{Sc} deposits in *tg*1020 mice but very little PrP^{Sc} stain in *tga20* mice, as shown by PrP immunohistochemistry (anti-PrP monoclonal antibody, SAF84). Histoblots of RL-RML also depict widespread distribution of PK-resistant PrP (PK concentration, 100 μg/ml). Scale bars: 200 μm (RL-RML); 500 μm (histoblot). (**E**) The correlation diagram of emission intensity of PTAA-bound PrP aggregates at wavelength ratios 531 nm/642 nm ($R_{531/642}$) and 531 nm/the emission maxima ($R_{531/Emax}$) shows the high variability of the RL-RML^1 in *tg*1020 mice. M-NS, mouse-adapted sheep scrapie. RL-RML^1 is a prion strain derived from RL mice infected with RML. (**F**) Westerns blots of the RL-RML^1 passage show homogeneous levels of PrP^{Sc} in *tg*1020 mice but heterogenous levels in *tga20* mice.

RML-PrP^{Sc} aggregates in brain displayed similar morphologies in *tga20* and *tg*1020 mice, consisting of widespread deposits visible by immunohistochemistry (Figure 2C). Elderly uninoculated *tg*1020 mice developed a spontaneous transmissible prion disease, with focal cerebral PrP plaques (53), yet the morphology of these spontaneous deposits was profoundly different from the widespread diffuse deposits developing in inoculated mice. Also, N-terminally cleaved PrP never acquired PK resistance of all 3 glycoforms in spontaneously sick *tg*1020 mice. Therefore, the PK-resistant PrP^{Sc} detected in *tg*1020 and *tga20* mice indicates that transmission of RML prions had occurred in both strains of host mice.

Inoculation of RL-RML^1 homogenate into a further generation of *tg*1020 mice resulted in a shortening of the ip and a reduction of variability by nearly 50%, to 171 ± 11 days (Figure 2, A and B, and Table 1). Hence, the substitutions of residues 170 and 174 had created a species barrier for RML prions, which was overcome by serial passaging. Conversely, back passage of the RL-RML^1 inoculum into *tga20* mice led to a more than 50% increase in the ip and to a 5-fold increase in variability (186 ± 33 days; Figure 2B and Table 1). The latter results point to a species barrier erected by the WT-*Prnp* sequence against RL-PrP prions. In conclusion, mouse prions could be adapted to hosts expressing either WT or RL *Prnp*; both resulting inocula were readily propagated in hosts

Table 1
Passage of mouse, deer, hamster, cattle, and sheep TSEs into mice expressing mouse PrP^C or RL-PrP^C

TSE	*tga20*		*tg*1020	
	Attack rate (no. infected/total)	ip (days)[A]	Attack rate (no. infected/total)	ip (days)[A]
RML[B]	4/4	74 ± 6	4/4	323 ± 92
RL-RML[1B]	6/6	186 ± 33	6/6	171 ± 11
CWD	4/4	543 ± 72	4/4	279 ± 48
RL-CWD	ND	–	4/4	401 ± 28
M-CWD	4/4	162 ± 6	4/4	252 ± 51
Hamster scrapie	1/4	449	6/6	468 ± 24
BSE	4/4	281 ± 139	0/4	–[C]
Sheep scrapie	4/4	405 ± 26	0/4	–[C]

[A]Mean ± SD. [B]RML infections were previously described (53). [C]Mice did not develop evidence of TSE. ND, not done.

expressing the same *Prnp* variant but were much less amenable to propagation in hosts expressing the other variant. This fulfills the definition of a species barrier.

RL-RML[1] PrP^{Sc} aggregates were sparsely distributed in *tga20* mice but were widespread in *tg*1020 mice, as shown by immunohistochemistry and histoblotting (Figure 2D). Neither RML nor RL-RML[1] tissue deposits were stained by Congo red (Supplemental Figure 1; supplemental material available online with this article; doi:10.1172/JCI42051DS1). We stained brain sections with the fluorescent amyloidotropic dye, polythiophene acetic acid (PTAA) (54). PTAA stains PrP^{Sc} deposits and emits distinct fluorescence spectra that report on the supramolecular arrangement of protein aggregates.

All RML-infected *tg*1020 brains, but none of the *tga20* brains, contained $PTAA^+$ plaques (Figure 2C). We compared PTAA emissions by plotting the fluorescence intensity ratio at 531 and 642 nm ($R_{531/642}$) against the ratio between the intensity at 531 nm and at the emission maximum ($R_{531/Emax}$). The resulting values are independent of absolute fluorescence intensity and can discriminate among multiple prion strains (55, 56). PTAA emission characteristics were highly variable among animals and sometimes even within individual animals, suggesting highly polymorphic PrP^{Sc} conformations in the first passage of RML (Figure 2E). However, none of the *tga20* and *tg*1020 mice inoculated with RL-RML[1] prions had $PTAA^+$ plaques. This finding suggests that the supramolecular arrangements of PrP^{Sc} had changed drastically upon passage.

We then compared brain homogenates of *tga20* and *tg*1020 mice inoculated with RL-RML[1] by PK digestion followed by Western blotting. The concentration of PrP^{Sc} was relatively homogenous in *tg*1020 mice but highly variable in *tga20* mice (Figure 2F). We concluded that the S170N and N174T substitutions created a species barrier to RML prions, which was eventually overcome in the RL mice through multiple passages.

Inoculation with CWD infectious brain homogenate. We then inoculated *tg*1020 and *tga20* mice with CWD prions from a terminal, naturally infected mule deer. WT mice are resistant to infection with CWD prions (57, 58), whereas overexpression of WT *Prnp* renders *tga20* mice susceptible to CWD — albeit after long ips (59). The mature PrP^C sequences of mice and mule deer differ at 23 residues, but the 165–175 loop sequence in *tg*1020 mice is identical to that of deer and elk (Figure 1A).

CWD infection led to accelerated disease in *tg*1020 mice compared with *tga20* mice (279 ± 48 days and 543 ± 72 days, respectively; Figure 3A and Table 1) (unpaired, 2-tailed Student's *t* test, $P = 0.001$). We detected abundant fine and clumped aggregates in hippocampus and cerebral cortex by using immunohistochemistry for PrP in *tg*1020 mice. The PTAA emission spectra were similar for all histologically visible aggregates in the first CWD passage, with little variability within and between *tg*1020 animals.

Surprisingly, the second passage of RL-CWD in *tg*1020 mice resulted in a slight lengthening of the ip (Figure 3A and Table 1). Using immunohistochemistry for PrP and PTAA emission spectra, 2 conspicuously differing PrP^{Sc} aggregate morphologies emerged: (a) a noncongophilic type, with a low $R_{531/642}$ similar to the first passage, and (b) a rare, 50- to 100-μm dense congophilic type, with a high $R_{531/642}$ (Figure 3B). The $R_{531/642}$, which depends on fluorescence resonance transfer between PTAA molecules, indicated that the LCP chains were tightly packed in the noncongophilic aggregates and loosely packed in the congophilic aggregates (Figure 3C). Maybe the conformational variants were interfering with the conversion of each other, thereby resulting in an unexpectedly long ip.

We then investigated the biochemical profile of CWD-induced PrP^{Sc} in *tg*1020 brain homogenates using PK digestion and PrP immunoblotting. The first passage of CWD in *tg*1020 mice yielded barely detectable PK-resistant PrP^{Sc}. By the second passage, PK-resistant PrP showed the typical shift in electrophoretic mobility, suggesting that a PK-resistant form had become more abundant (Figure 3D).

We then assessed the effect of the PrP^{Sc} primary amino acid sequence on the strain properties by comparing a mouse-adapted CWD (M-CWD) strain with mule deer CWD in *tg*1020 mice. There was no significant difference in the ips: M-CWD–infected *tg*1020 mice (Figure 3E) and mule deer CWD–infected *tg*1020 mice (Figure 3A) had ips of 252 ± 51 days and 279 ± 48 days, respectively (Student's *t* test, $P = 0.45$).

PrP aggregates in the M-CWD–inoculated *tg*1020 brains histologically appeared large and congophilic (Figure 3F), similar to the rare congophilic plaques seen in the RL-CWD–infected *tg*1020 mice and the M-CWD–infected *tga20* mice (Figure 3, B and F). The LCP emission spectra $R_{531/642}$ and $R_{531/Emax}$ were also similar (Figure 3G), with values that are indicative of loosely packed PTAA chains.

The above data indicate that after primary deer CWD inoculation, RL-PrP may give rise to morphologically small, noncongophilic aggregates, leading to tight packing of PTAA, or large, congophilic plaques, leading to looser packing of PTAA. In contrast, the M-CWD strain gave rise to a single morphology in both *tga20* and *tg*1020 mice, which appeared similar to the large congophilic plaques described above.

Inoculation of hamster scrapie into RL-PrP and WT-PrP mice. Mice were initially believed to be completely resistant to infection with particular strains of hamster prions (60), but an extensive series of experiments revealed that mice can replicate hamster prions subclinically (32). The hamster PrP^C β_2-α_2 loop sequence is homologous with the RL-PrP sequence at position 170N and with

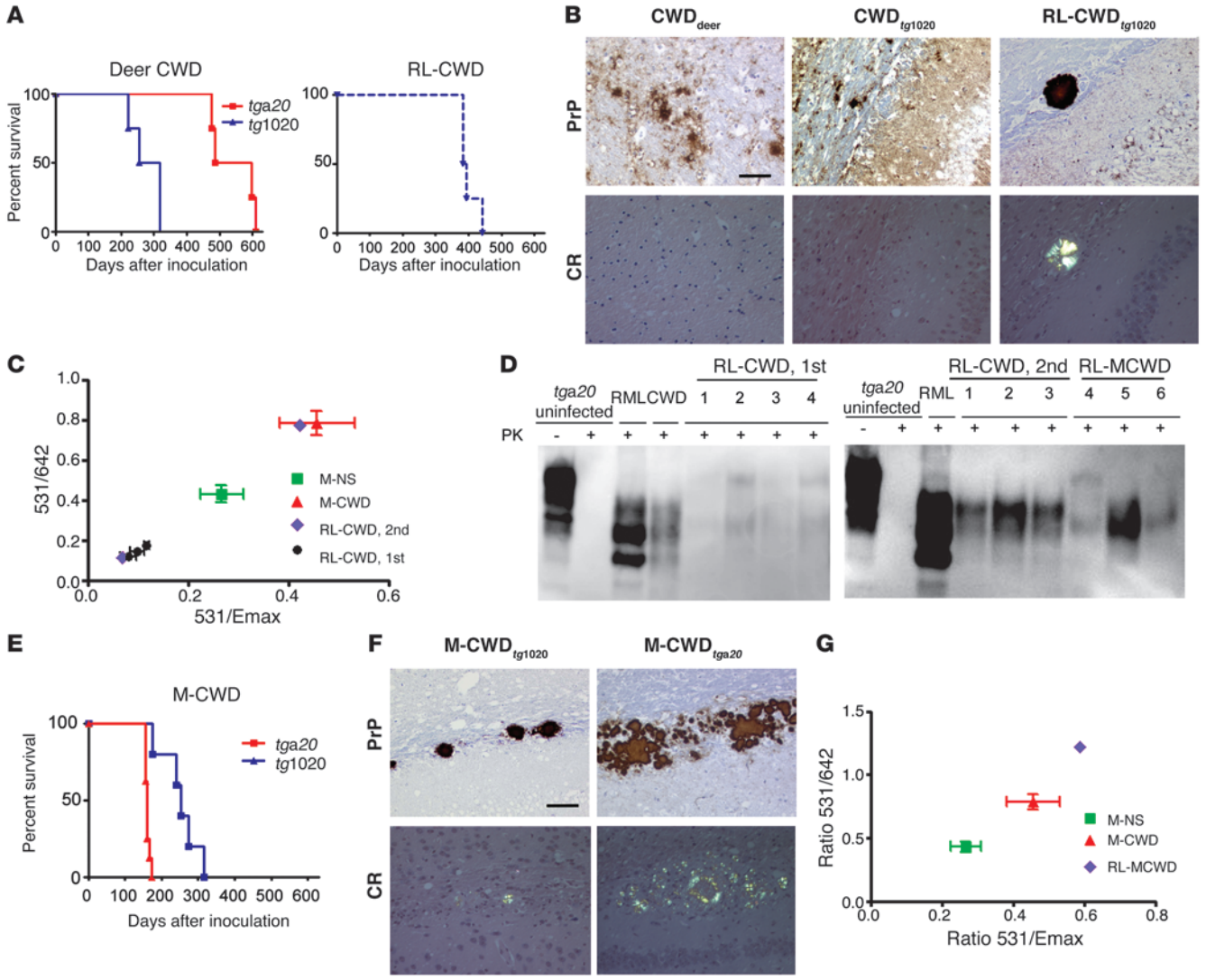

Figure 3

Mule deer CWD infection of *tga20* and *tg*1020 mice. (**A**) A survival curve of *tga20* and *tg*1020 mice infected with mule deer CWD shows a shorter and less variable ip in *tg*1020 mice (blue line), which was slightly longer on second passage (referred to as RL-CWD). (**B**) Similar to deer, CWD-PrP^{Sc} aggregates in *tg*1020 mice on first passage are small, irregular, and noncongophilic (middle panel). Upon second passage, large unicentric, congophilic plaques emerge (RL-CWD, right panel). Cr, Congo red. (**C**) The first passage of CWD in *tg*1020 mice (RL-CWD, 1st; black circles) shows a highly consistent emission profile of PTAA-bound PrP aggregates, whereas on second passage (RL-CWD, 2nd; purple diamonds), both the emission ratio from the first passage and a new ratio from the congophilic plaques emerge. Murine-adapted sheep scrapie (green square) and M-CWD (red triangle) in *tga20* mice are also shown for comparison. (**D**) CWD in *tg*1020 was primarily PK sensitive on the first passage in *tg*1020 mice. By the second passage, RL-CWD was PK-resistant (lanes 1–3). M-CWD in *tg*1020 mice showed weakly PK-resistant PrP (lanes 4–6). (**E**) *tg*1020 mice inoculated with M-CWD have a slightly longer and more variable ip, as compared with the *tga20* mice. (**F**) PrP aggregates of M-CWD in *tg*1020 and *tga20* mice are similarly dense and congophilic. (**G**) The PTAA emission ratio of M-CWD inoculated into the *tg*1020 mice (RL-MCWD, purple diamond) is more closely similar to that of M-CWD in *tga20* mice than to that of murine-adapted sheep scrapie in *tga20* mice. Scale bars: 50 μm.

the WT mouse sequence at 174N. To determine whether either WT-PrP or RL-PrP, or both, could support hamster prion replication, we inoculated *tga20* and *tg*1020 mice with the Sc237 strain of hamster prions. The ips were consistently more than 400 days for all mice, but the attack rate varied markedly. Whereas 6 out of 6 *tg*1020 mice showed N-terminally cleaved, PK-resistant PrP^{Sc} accumulation in histoblot and Western blot assays (Figure 4, A and B), versus a background of 0 out of 13 uninoculated *tg*1020 mice (Supplemental Figure 2), only 1 out of 4 *tga20* mice had any detectable PrP^{Sc}, even following concentration of PrP^{Sc} by sodium phosphotungstic acid precipitation (Figure 4B). *tg*1020 mice, but not *tga20* mice, showed conspicuous spongiform encephalopathy, which was particularly evident in the cerebral cortex (Figure 4C). PrP^{Sc} aggregates were finely granular and diffusely distributed (Figure 4A). The Congo red, PTAA, and polythiophene methyl imidazole (PTMI) stains were negative (Supplemental Figures 1 and 3), precluding emission spectra comparisons with RL-RML or RL-CWD. We concluded that hamster scrapie could be con-

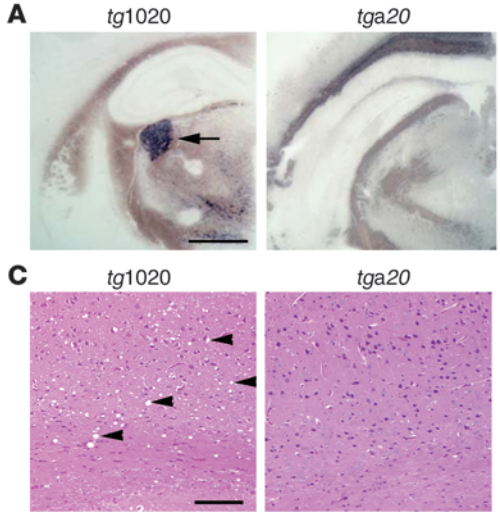

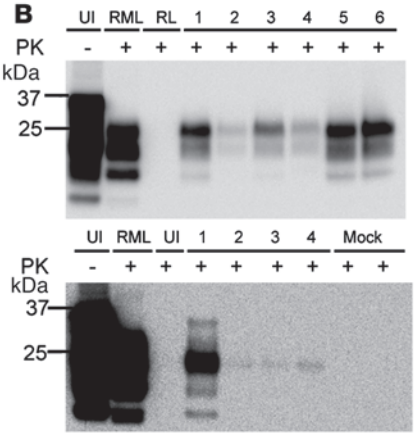

Figure 4
Hamster scrapie infects *tg*1020 mice. (**A**) PK-resistant PrP is clearly evident in the frozen brain sections of *tg*1020 mice (arrow) but not *tga20* mice. Scale bar: 1 mm. (**B**) PrP^{Sc} is predominantly diglycosylated and present in 6 out of 6 *tg*1020 (top panel) mice infected with hamster scrapie, but it is seen in only 1 out of 4 *tga20* mice (bottom panel). UI, uninfected. (**C**) The cerebral cortex of *tg*1020 and *tga20* mice infected with hamster scrapie shows extensive spongiform degeneration in the *tg*1020 mice (denoted by arrowheads). Scale bar: 100 μm.

sistently transmitted to *tg*1020 but not *tga20* mice. The long ip suggests either inefficient transmission or generation of PrP^{Sc} aggregates with low toxicity.

Inoculation with BSE and sheep scrapie. We inoculated *tg*1020 and *tga20* mice with BSE and sheep scrapie isolates (Swiss BSE and Colorado sheep scrapie from single animals). Cattle, sheep, and mouse PrP protein sequences are identical at the β_2-α_2 loop, and both BSE and sheep scrapie isolates can infect *tga20* mice, as previously reported (56). After inoculation with BSE or sheep scrapie, aged *tg*1020 mice (>300 days old) developed weight loss and mild paraparesis as well as rare RL-PrP plaques in the hippocampus. However, in the *tg*1020 mice there was no evidence for BSE or sheep scrapie transmission by any method. PrP histoblots and Western blots were consistently negative for PK-resistant PrP^{Sc} (Supplemental Figures 2 and 4).

In vitro cross-species PrP^{Sc} amplification using protein misfolding cyclic amplification. To assess whether the transmission barrier induced by the S170N and N174T substitutions could be reproduced in vitro, we performed protein misfolding cyclic amplification (PMCA) experiments, using the *tg*1020 and *tga20* brain as a substrate. We seeded the PMCA reaction with RML mouse prions, 263K hamster scrapie, deer CWD, and Colorado sheep scrapie. Six separate samples of *tg*1020 and *tga20* brain were seeded with each prion strain and amplified for 5 rounds (Table 2 and Supplemental Figure 5). We found that by the fifth round, *tg*1020 brain homogenates yielded PK-resistant PrP in 100% of samples seeded with hamster scrapie and 83% of samples seeded with CWD, compared with only 17% and 50% of *tga20* brain homogenates seeded with hamster scrapie and CWD, respectively. *tg*1020 and *tga20* brain homogenate led to PK-resistant PrP in all samples seeded with RML but in no samples seeded with sheep scrapie. Therefore, the PMCA experiments largely reproduced our in vivo findings; the main difference occurred with sheep scrapie, in which PK-resistant PrP^{Sc} was not detected in any of the *tga20* and *tg*1020 samples. Although we have shown that the *tga20* mice and *tg*1020 mice were both susceptible to RML infection, the difference in the ip was not revealed by differences in seeding ability using PMCA.

Discussion

170 and 174 are positions that can modulate prion transmission. The S170N and N174T substitutions in the β_2-α_2 loop of PrP^{C} erected a complete barrier to TSEs derived from 2 different host species, cattle and sheep (Table 3). Conversely, the very strong barrier of mice against hamster prions was completely ablated, as hamster prions infected all mice expressing RL-PrP^{C} (Table 3). The potent impact on species barriers caused by 2 amino acid substitutions indicates that prion species barriers may be profoundly altered in humans or animals expressing polymorphisms or mutant PrP molecules. Thus, human or animal TSEs may be replicated by mutant molecules, even when otherwise strong species barriers are known to exist.

TSE infection in the tg1020 mice. We have previously reported that *tg*1020 mice spontaneously develop a new strain of TSE (53). The resulting disease may confound the assessment of TSE transmission to prion-inoculated *tg*1020 mice. On the other hand, several traits allowed for unequivocal differentiation between transmitted and spontaneous prion disease. First, immunoblots showed the canonical "shift" in electrophoretic mobility in PrP^{Sc} recovered from TSE-infected *tg*1020 mice after PK digestion. This shift has never been detected in spontaneously sick *tg*1020 mice. Second, inoculated mice showed widespread deposition of PrP^{Sc} in the brain, which extended to regions, such as the thalamus, in which aggregates have never been observed in spontaneous disease. Third, the staining profiles of specific LCP dyes and their fluorescence emission spectra differed vastly between inoculated and spontaneously sick *tg*1020 mice. For example, PTAA failed to stain any brain sections of RL-RML[2] and RL hamster strains in *tg*1020 mice, whereas it consistently labeled spontaneously appearing prion aggregates. Taken together, these features support that the instances of disease reported in this study represent bona fide transmission of TSE rather than spontaneous disease typical of noninoculated *tg*1020 mice.

tga20 mice express 2-fold more PrP^{C} than the *tg*1020 mice and would therefore have been expected to develop prion disease after a shorter ip if there was no transmission barrier induced by the S170N and N174T substitutions. However, the *tga20* mice only developed prion disease with a shorter ip after inoculation with RML prions and actually had a longer ip after inoculation with CWD prions. With RML infection, the *tg*1020 mice showed clear evidence of a transmission barrier, in that the ip exceeded that of lower expressing WT mice and shortened by 50% upon second passage. Together, the data clearly support that the differences

Table 2
Serial automated PMCA using *tg*1020 brain homogenate as the substrate

Passage	P3 (no. PrP^{Sc}-positive tubes/total)		P4 (no. PrP^{Sc}-positive tubes/total)		P5 (no. PrP^{Sc}-positive tubes/total)	
	tga20	*tg*1020	*tga20*	*tg*1020	*tga20*	*tg*1020
Unseeded	0/6	0/6	0/6	0/6	0/6	0/6
RML	6/6	6/6	6/6	6/6	6/6	6/6
Hamster scrapie	0/6	1/6	0/6	5/6	1/6	6/6
Deer CWD	1/6	2/6	3/6	3/6	3/6	5/6
Sheep scrapie	0/6	0/6	0/6	0/6	0/6	0/6

Brains from *tg*1020 and *tga20* mice were extracted after perfusion with PBS plus 5 mM EDTA and used as substrate or source of PrP^C. Sixty μl of brain homogenates were treated in replicates of 6 ($n = 6$) with serial automated PMCA (91, 92) and were incubated/sonicated for 48 hours in each round. After each round of PMCA, the PK-resistant PrP (PrP^{Sc}) in the sonicated/incubated samples was analyzed by Western blotting and diluted 1:10 into a freshly prepared *tg*1020 or *tga20* mouse brain homogenate to start the next PMCA round (from P1 to P5). This process was repeated for 5 rounds (P5). The fraction of PrP^{Sc}-positive tubes is indicated for rounds P3 to P5 of PMCA.

in prion susceptibility are due to the S170N and N174T substitutions and not due to the differences in PrP^C expression.

Consistency of in vivo and in vitro studies of species barriers. Two decades of published studies indicate that the penetrance of cross-species transmission is affected by the sequence similarity between the host PrP^C and the incoming PrP^{Sc} (61). Even single–amino acid polymorphisms can radically alter the transmissibility profiles of individual prion strains (62–69). Scrapie infection of cells expressing variant sequences of PrP^C has also revealed the striking effects of mutations on the efficiency of conversion of PrP^C to PrP^{Sc} (70).

Hamster prions were successfully transmitted only to *tg*1020 mice and not to *tga20* mice. The hamster PrP sequence is homologous to RL-PrP at position 170 and to WT-PrP at position 174, suggesting that homology at 170 was critical for transmission. Studies of prion transmission in bank voles and PMCA experiments with CWD in a panel of mammalian species also implicate residue 170 as a key position for influencing species barriers (37, 71). These results can be rationalized by classifying TSE hosts into 2 groups: 170S animals that include cattle, sheep, and mice and 170N animals that include elk, deer, hamsters, and RL mice.

Here, we show that susceptibility to a number of prion strains seemed to be driven by homology at position 170, although further experiments with single mutants would be necessary to fully clarify the relative contributions of residues at positions 170 and 174. *tga20* mice could readily convert other 170S prions, such as cattle BSE and classical sheep scrapie, but not the 170N prions, such as hamster scrapie. While the overexpressing *tga20* mice could convert 170N mule deer CWD prions after a long ip (59), WT mice are resistant to CWD (57, 58). Conversely, *tg*1020 mice could convert 170N hamster scrapie and mule deer CWD but completely resisted infection with 170S sheep scrapie and BSE (Table 3). While *tg*1020 mice may have developed spontaneous infectivity, which would have been detected on further passages, this possibility would not have interfered with the above interpretation.

The above results prompted us to reinterpret published prion transmission experiments and epidemiologic studies in the context of the 170S/170N transmission barrier. In accordance with our predictions, prions are readily transmitted within 170S mammals: sheep scrapie prions infect cattle (72–74) and mice (75, 76), and cattle BSE prions readily infect sheep (77–79) and mice (14, 80). BSE (170S) has also been transmitted to other 170S species, including greater kudu, nyala, eland, scimitar-horned oryx, bison, rhesus macaque, domestic cat, and mink (13, 16, 81, 82). Conversely, prions generated in 170S animals are poorly transmissible to 170N recipients and vice versa. Transgenic mice overexpressing bovine or ovine PrP completely resisted infection to 9 different CWD isolates (58), and WT mice do not develop clinical prion disease after infection with elk CWD or hamster 263K scrapie (57, 58, 60). Furthermore, cattle and sheep are poorly infectible with mule deer CWD, since few animals develop disease after prolonged ips of 6 years, and only after intracerebral inoculation (83, 84). Among 170N animals, prions are also transmissible, as elk CWD is infectious to hamsters (85), albeit not very efficiently. Collectively, most historical data from studies on species barriers support the model that similarity at the loop region, and particularly the 170S/N switch, impacts transmission barriers in a broad variety of species. As a possible exception to these observations, cattle may be susceptible to CWD from white-tailed deer (86). The latter finding suggests that specific prion strains can overrule the codon 170 homology requirement.

Does the β_2-α_2 loop direct prion strain conformation? What are the structural consequences of the substitutions at residues 170 and 174, and how might they explain the important role of these substitutions in interspecies prion transmission? Crystallographic investigations of PrP peptides revealed that adjacent β_2-α_2 loops can engage in a "dry steric zipper" interface, which was proposed to represent the elemental backbone of many amyloids. Peptide crystal structures encompassing the β_2-α_2 loops bearing the 170S/174N and 170N/174T substitutions were arranged in a

Table 3
Interspecies transmission of TSEs in *tga20* and *tg*1020 mice, as determined by PK-resistant PrP^{Sc} in brain

TSE origin	Transmission to *tga20* mice	Transmission to *tg*1020 mice
Mouse	+	+
Deer	+[A]	+
Hamster	+/–[B]	+
Cattle	+	–
Sheep	+	–

[A]WT mice are resistant (57). [B]One out of four mice developed PrP aggregates in brain. Infection with prions is indicated by "+" and no infection is indicated by "–".

P1 or a $P2_1$ crystal space group, respectively (87). These observations suggest striking differences in the β-sheet alignment of PrP^{Sc} aggregates between prion-infected 170S and 170N animals and may provide a plausible starting point for clarifying the structural basis of prion species barriers that are highly relevant to public health, including the potential transmissibility of bovine and cervid prions to humans.

Methods

Prion inoculations. *tga20* or *tg*1020 (RL) transgenic mice, which overexpressed murine PrP (52, 53), were intracerebrally inoculated in the left parietal cortex with 30 μl of brain homogenate. This was either a 5%–10% brain homogenate from a terminally sick, naturally CWD-infected mule deer (provided by M. Miller, Colorado Division of Wildlife, Fort Collins, Colorado, USA), an uninfected control deer (reported in ref. 59), a 5% brain homogenate from a terminal, naturally scrapie-infected Suffolk sheep (n = 4 mice) (provided by T. Spraker, Colorado State University, Fort Collins, Colorado, USA), or a 5% brain homogenate from a naturally BSE-infected cow (n = 4 mice) (provided by A. Zurbriggen, University of Bern, Bern, Switzerland). Mice were monitored every second day, and TSE was diagnosed according to clinical criteria, including ataxia, kyphosis, and hind leg paresis. Mice were sacrificed at the onset of terminal disease. Mice were maintained under specific pathogen–free conditions. All of the present studies were reviewed and approved by the animal care and use committee (Kantonales Veterinäramt Zürich) in the Zurich Cantonal Veterinary Office, Switzerland.

Western blots. The 10% brain or spleen homogenates were prepared in PBS, using a Precellys 24 Tissue Homogenizer. Extracts of 50–90 μg protein were diluted with a Tris-based buffer (10 mM Tris, 10 mM EDTA, 100 mM NaCl, 0.5% NP40, and 0.5% DOC) and digested with 100 μg/ml PK for 30 minutes at 37°C. A SDS-based buffer was then added, and the samples were heated to 95°C for 5 minutes, prior to electrophoresis through a 12% Bis-Tris precast gel (Invitrogen), followed by transfer to a nitrocellulose membrane by wet blotting. Proteins were detected with anti-PrP POM1 antibody (epitope in the globular domain, amino acids 121–231) (88). For secondary detection, we used an HRP-conjugated anti-mouse IgG antibody (Zymed, Invitrogen). Signals were visualized with the ECL detection kit (Pierce). Sodium phosphotungstic acid (NaPTA) precipitation was used when noted to enrich for PrP^{Sc}, prior to Western blotting, using published methods (89).

Histoblots. Histoblots were performed as reported in Taraboulos et al. (90), using up to 100 μg/ml of PK for the digestion of PrP^{C}. Histoblots were developed using the anti-PrP POM1 antibody (88).

PTAA staining of frozen tissue sections. Frozen sections from mouse brain were dried for 1 hour and fixed in 100% and 70% ethanol for 10 minutes each. After washing with deionized water, sections were equilibrated in 100 mM sodium carbonate at pH 10.2 for 30 minutes. The PTAA was diluted in the sodium carbonate buffer (1 μg per 100 μl buffer) and added to the sections. The sections were incubated with PTAA for 30 minutes at room temperature and washed with sodium carbonate buffer. The spectra in the tissue were recorded with a Zeiss Axioplan 2 microscope, fitted with a Spectraview 4.0 (Applied Spectral Imaging) and a Spectra-Cube (interferometrical optical head SD 300) module with cooled CCD camera, through a 470 nm/40 nm (LP 515) bandpass filter (Zeiss) in steps of 10 nm. The data were processed with SpectraView 3.0 EXPO. Spectra were collected from 10 individual spots within 3–4 plaques, from a minimum of 3 different mice of each prion strain.

PTAA staining of formalin-fixed tissue sections. Paraffin-embedded, formalin-fixed, and formic-acid treated brain sections were deparaffinized and treated with PK (10 μg/ml in PBS) for 10 minutes prior to staining. PTAA staining was performed as described above.

Histopathology and immunohistochemical stains. Two-μm-thick sections were cut onto positively charged silanized glass slides and stained with H&E or immunostained using antibodies for PrP (SAF84), for astrocytes (GFAP), or microglia (Iba1). For PrP staining, sections were deparaffinized, incubated for 6 minutes in 98% formic acid, and then washed in distilled water for 5 minutes. Sections were heated to 100°C in a pressure cooker in citrate buffer (pH 6.0), cooled for 3 minutes, and washed in distilled water for 5 minutes. Immunohistochemical stains were performed on an automated Nexus staining apparatus (Ventana Medical Systems), using an iVIEW DAB Detection Kit (Ventana Medical Systems). After incubation with protease 1 (Ventana Medical Systems) for 16 minutes, sections were incubated with anti-PrP SAF-84 (SPI-bio; 1:200) for 32 minutes. Sections were counterstained with hematoxylin. GFAP immunohistochemistry (1:1,000 for 24 minutes; DAKO) for astrocytes and Iba1 immunohistochemistry (1:2,500 for 32 minutes; Wako Chemicals) for microglia were similarly performed, but with antigen retrieval, by heating to 100°C in EDTA buffer (pH 8.0).

Serial automated PMCA procedure. The whole process of in vitro prion replication, including the PrP^{Sc} detection of amplified samples, was performed following the basic conditions described previously (91–93). The optimization of the technique was performed empirically, taking into account all modifiable parameters. Our optimal results were obtained using the following settings: 60 μl of sample, 70% of power of sonication, 30 minutes of incubation time, 20 seconds of constant sonication, 180 ml of water over the horn plate sonicator, and 37°C–38°C in the water of sonication.

Statistics. Continuous data are presented as mean ± SD. The ips, from inoculation to terminal prion disease, in the *tga20* and *tg*1020 mice were compared using Student's unpaired t test. Two-tailed P values of less than 0.05 were considered significant. Statistical analyses were performed using GraphPad Prism.

Acknowledgments

We thank our histopathology and animal care staff for technical support. This study was supported by the European Union (TSEUR to A. Aguzzi and UPMAN to K. Wüthrich), the Swiss National Science Foundation, the National Competence Centers for Research on Neural Plasticity and Repair (to A. Aguzzi) and on Structural Biology (to K. Wüthrich), NIH grants K08-AI01802 and 5R21NS055116 (to C.J. Sigurdson), the Foundation for Research at the University of Zürich (to C.J. Sigurdson), the US National Prion Research Program (to C.J. Sigurdson and A. Aguzzi), the Knut and Alice Wallenberg Foundation (to K.P.R. Nilsson), and the ETH Zürich (to K. Wüthrich). K. Wüthrich is the Cecil H. and Ida M. Green Professor of Structural Biology at The Scripps Research Institute.

Received for publication December 15, 2009, and accepted in revised form April 28, 2010.

Address correspondence to: Adriano Aguzzi, UniversitätsSpital Zürich, Institute of Neuropathology, Department of Pathology, Schmelzbergstrasse 12, CH–8091 Zürich, Switzerland. Phone: 41.44.255.2107; Fax: 41.44.255.4402; E-mail: adriano.aguzzi@usz.ch. Or to: Christina Sigurdson, Department of Pathology, University of California, San Diego, 9500 Gilman Dr., La Jolla, California 92093, USA. Phone: 858.534.0978; Fax: 858.246.0523; E-mail: csigurdson@ucsd.edu.

K. Peter R. Nilsson's present address is: Department of Chemistry, IFM, Linköping University, Linköping, Sweden.

Simone Hornemann's present address is: UniversitätsSpital Zürich, Institute of Neuropathology, Zürich, Switzerland.

1. Aguzzi A. Understanding the diversity of prions. *Nat Cell Biol*. 2004;6(4):290–292.
2. Prusiner SB. Novel proteinaceous infectious particles cause scrapie. *Science*. 1982;216(4542):136–144.
3. Prusiner SB. Molecular biology of prion diseases. *Science*. 1991;252(5012):1515–1522.
4. Collinge J, Clarke AR. A general model of prion strains and their pathogenicity. *Science*. 2007;318(5852):930–936.
5. Fraser H, Dickinson AG. The sequential development of the brain lesion of scrapie in three strains of mice. *J Comp Pathol*. 1968;78(3):301–311.
6. Fraser H, Dickinson AG. Scrapie in mice. Agent-strain differences in the distribution and intensity of grey matter vacuolation. *J Comp Pathol*. 1973;83(1):29–40.
7. Bruce ME, McBride PA, Farquhar CF. Precise targeting of the pathology of the sialoglycoprotein, PrP, and vacuolar degeneration in mouse scrapie. *Neurosci Lett*. 1989;102(1):1–6.
8. Bessen RA, Marsh RF. Biochemical and physical properties of the prion protein from two strains of the transmissible mink encephalopathy agent. *J Virol*. 1992;66(4):2096–2101.
9. Hill AF, et al. Distinct glycoform ratios of protease resistant prion protein associated with *PRNP* point mutations. *Brain*. 2006;129(pt 3):676–685.
10. Safar J, et al. Eight prion strains have PrP^{Sc} molecules with different conformations. *Nature Medicine*. 1998;4(10):1157–1165.
11. Peretz D, et al. A change in the conformation of prions accompanies the emergence of a new prion strain. *Neuron*. 2002;34(6):921–932.
12. Will RG, et al. A new variant of Creutzfeldt-Jakob disease in the UK. *Lancet*. 1996;347(9006):921–925.
13. Collinge J, Sidle KC, Meads J, Ironside J, Hill AF. Molecular analysis of prion strain variation and the aetiology of 'new variant' CJD. *Nature*. 1996;383(6602):685–690.
14. Bruce ME, et al. Transmissions to mice indicate that 'new variant' CJD is caused by the BSE agent *Nature*. 1997;389(6650):498–501.
15. Seitz R, et al. Impact of vCJD on blood supply. *Biologicals*. 2007;35(2):79–97.
16. Kirkwood JK, Cunningham AA. Epidemiological observations on spongiform encephalopathies in captive wild animals in the British Isles *Vet Rec*. 1994;135(13):296–303.
17. Ryder SJ, Wells GA, Bradshaw JM, Pearson GR. Inconsistent detection of PrP in extraneural tissues of cats with feline spongiform encephalopathy. *Vet Rec*. 2001;148(14):437–441.
18. Kirkwood JK, Cunningham AA, Wells GA, Wilesmith JW, Barnett JE. Spongiform encephalopathy in a herd of greater kudu (Tragelaphus strepsiceros): epidemiological observations. *Vet Rec*. 1993;133(15):360–364.
19. Sigurdson CJ, Miller MW. Other animal prion diseases. *Br Med Bull*. 2003;66:199–212.
20. Pattison IH, Jones KM. Modification of a strain of mouse-adapted scrapie by passage through rats. *Res Vet Sci*. 1968;9(5):408–410.
21. Benestad SL, Sarradin P, Thu B, Schonheit J, Tranulis MA, Bratberg B. Cases of scrapie with unusual features in Norway and designation of a new type, Nor98. *Vet Rec*. 2003;153(7):202–208.
22. Sofianidis G, Psychas V, Billinis C, Spyrou V, Argyroudis S, Vlemmas I. Atypical PrP^{Sc} distribution in goats naturally affected with scrapie. *J Comp Pathol*. 2008;138(2–3):90–101.
23. Biacabe AG, Laplanche JL, Ryder S, Baron T. Distinct molecular phenotypes in bovine prion diseases. *EMBO Rep*. 2004;5(1):110–115.
24. Casalone C, et al. Identification of a second bovine amyloidotic spongiform encephalopathy: molecular similarities with sporadic Creutzfeldt-Jakob disease. *Proc Natl Acad Sci U S A*. 2004;101(9):3065–3070.
25. Telling GC, et al. Transmission of Creutzfeldt-Jakob disease from humans to transgenic mice expressing chimeric human-mouse prion protein. *Proc Natl Acad Sci U S A*. 1994;91(21):9936–9940.
26. Telling GC, et al. Prion propagation in mice expressing human and chimeric PrP transgenes implicates the interaction of cellular PrP with another protein. *Cell*. 1995;83(1):79–90.
27. Priola SA, Chesebro B. A single hamster PrP amino acid blocks conversion to protease-resistant PrP in scrapie-infected mouse neuroblastoma cells. *J Virol*. 1995;69(12):7754–7758.
28. Horiuchi M, Priola SA, Chabry J, Caughey B. Interactions between heterologous forms of prion protein: binding, inhibition of conversion, and species barriers. *Proc Natl Acad Sci U S A*. 2000;97(11):5836–5841.
29. Kocisko DA, Priola SA, Raymond GJ, Chesebro B, Lansbury PT Jr, Caughey B. Species specificity in the cell-free conversion of prion protein to protease-resistant forms: a model for the scrapie species barrier. *Proc Natl Acad Sci U S A*. 1995;92(9):3923–3927.
30. Scott M, et al. Transgenic mice expressing hamster prion protein produce species-specific scrapie infectivity and amyloid plaques. *Cell*. 1989;59(5):847–857.
31. Prusiner SB, et al. Transgenetic studies implicate interactions between homologous PrP isoforms in scrapie prion replication. *Cell*. 1990;63(4):673–686.
32. Race R, Meade-White K, Raines A, Raymond GJ, Caughey B, Chesebro B. Subclinical scrapie infection in a resistant species: persistence, replication, and adaptation of infectivity during four passages. *J Infect Dis*. 2002;186(suppl 2):S166–S170.
33. Barron RM, et al. Changing a single amino acid in the N-terminus of murine PrP alters TSE incubation time across three species barriers. *EMBO J*. 2001;20(18):5070–5078.
34. Barron RM, Manson JC. A gene-targeted mouse model of P102L Gerstmann-Sträussler-Scheinker syndrome. *Clin Lab Med*. 2003;23(1):161–173.
35. Collinge J, Beck J, Campbell T, Estibeiro K, Will RG. Prion protein gene analysis in new variant cases of Creutzfeldt-Jakob disease. *Lancet*. 1996;348(9019):56.
36. Nonno R, et al. Efficient transmission and characterization of Creutzfeldt-Jakob disease strains in bank voles. *PLoS Pathog*. 2006;2(2):e12.
37. Piening N, et al. Conversion efficiency of bank vole prion protein in vitro is determined by residues 155 and 170, but does not correlate with the high susceptibility of bank voles to sheep scrapie in vivo. *J Biol Chem*. 2006;281(14):9373–9384.
38. Wopfner F, et al. Analysis of 27 mammalian and 9 avian PrPs reveals high conservation of flexible regions of the prion protein. *J Mol Biol*. 1999;289(5):1163–1178.
39. Billeter M, Riek R, Wider G, Hornemann S, Glockshuber R, Wüthrich K. Prion protein NMR structure and species barrier for prion diseases. *Proc Natl Acad Sci U S A*. 1997;94(14):7281–7285.
40. Riek R, Hornemann S, Wider G, Billeter M, Glockshuber R, Wüthrich K. NMR Structure of the Mouse Prion Protein Domain Prp(121–231). *Nature*. 1996;382(6587):180–182.
41. Gorfe AA, Caflisch A. Ser170 controls the conformational multiplicity of the loop 166-175 in prion proteins: implication for conversion and species barrier. *FASEB J*. 2007;21(12):3279–3287.
42. Riek R, Hornemann S, Wider G, Glockshuber R, Wüthrich K. NMR characterization of the full-length recombinant murine prion protein, mPrP(23–231). *FEBS Lett*. 1997;413(2):282–288.
43. Hornemann S, Schorn C, Wüthrich K. NMR structure of the bovine prion protein isolated from healthy calf brains. *EMBO Rep*. 2004;5(12):1159–1164.
44. Liu H, et al. Solution structure of Syrian hamster prion protein rPrP(90–231). *Biochemistry*. 1999;38(17):5362–5377.
45. Lopez Garcia F, Zahn R, Riek R, Wüthrich K. NMR structure of the bovine prion protein. *Proc Natl Acad Sci U S A*. 2000;97(15):8334–8339.
46. Lysek DA, et al. Prion protein NMR structures of cats, dogs, pigs, and sheep. *Proc Natl Acad Sci U S A*. 2005;102(3):640–645.
47. Zahn R, et al. NMR solution structure of the human prion protein. *Proc Natl Acad Sci U S A*. 2000;97(1):145–150.
48. Schätzl HM, Da Costa M, Taylor L, Cohen FE, Prusiner SB. Prion protein gene variation among primates. *J Mol Biol*. 1995;245(4):362–374.
49. Christen B, Hornemann S, Damberger FF, Wüthrich K. Prion protein NMR structure from tammar wallaby (Macropus eugenii) shows that the beta2-alpha2 loop is modulated by long-range sequence effects. *J Mol Biol*. 2009;389(5):833–845.
50. Christen B, Perez DR, Hornemann S, Wüthrich K. NMR structure of the bank vole prion protein at 20 degrees C contains a structured loop of residues 165-171. *J Mol Biol*. 2008;383(2):306–312.
51. Gossert AD, Bonjour S, Lysek DA, Fiorito F, Wüthrich K. Prion protein NMR structures of elk and of mouse/elk hybrids. *Proc Natl Acad Sci U S A*. 2005;102(3):646–650.
52. Fischer M, et al. Prion protein (PrP) with amino-proximal deletions restoring susceptibility of PrP knockout mice to scrapie. *EMBO J*. 1996;15(6):1255–1264.
53. Sigurdson CJ, et al. De novo generation of a transmissible spongiform encephalopathy by mouse transgenesis. *Proc Natl Acad Sci U S A*. 2009;106(1):304–309.
54. Ding L, Jonforsen M, Roman LS, Andersson MR, Inganas O. Photovoltaic cells with a conjugated polyelectrolyte. *Synth Met*. 2000;110(2):133–140.
55. Nilsson KPR, et al. Imaging distinct conformational states of amyloid-beta fibrils in Alzheimer's disease using novel luminescent probes. *ACS Chem Biol*. 2007;2(8):553–560.
56. Sigurdson CJ, et al. Prion strain discrimination using luminescent conjugated polymers. *Nat Methods*. 2007;4(12):1023–1030.
57. Browning SR, et al. Transmission of prions from mule deer and elk with chronic wasting disease to transgenic mice expressing cervid PrP. *J Virol*. 2004;78(23):13345–13350.
58. Tamguney G, et al. Transmission of elk and deer prions to transgenic mice. *J Virol*. 2006;80(18):9104–9114.
59. Sigurdson CJ, et al. Strain fidelity of chronic wasting disease upon murine adaptation. *J Virol*. 2006;80(24):12303–12311.
60. Kimberlin RH, Walker CA. Evidence that the transmission of one source of scrapie agent to hamsters involves separation of agent strains from a mixture. *J Gen Virol*. 1978;39(3):487–496.
61. Scott M, et al. Propagation of prions with artificial properties in transgenic mice expressing chimeric PrP genes. *Cell*. 1993;73(5):979–988.
62. Moore RC, et al. Mice with gene targetted prion protein alterations show that Prnp, Sinc and Prni are congruent. *Nat Genet*. 1998;18(2):118–125.
63. Wadsworth JD, Collinge J. Update on human prion disease. *Biochim Biophys Acta*. 2007;1772(6):598–609.
64. O'Rourke KI, et al. PrP genotypes of captive and free-ranging Rocky Mountain elk (Cervus elaphus nelsoni) with chronic wasting disease. *J Gen Virol*. 1999;80(pt 10):2765–2769.
65. Jewell JE, Conner MM, Wolfe LL, Miller MW, Williams ES. Low frequency of PrP genotype 225SF among free-ranging mule deer (Odocoileus hemionus) with chronic wasting disease. *J Gen Virol*. 2005;86(pt 8):2127–2134.
66. Johnson C, Johnson J, Vanderloo JP, Keane D, Aiken JM, McKenzie D. Prion protein polymorphisms in white-tailed deer influence susceptibility to chronic wasting disease. *J Gen Virol*. 2006;87(pt 7):2109–2114.

67. Meade-White K, et al. Resistance to chronic wasting disease in transgenic mice expressing a naturally occurring allelic variant of deer prion protein. *J Virol*. 2007;81(9):4533–4539.
68. Jones EM, Surewicz WK. Fibril conformation as the basis of species- and strain-dependent seeding specificity of mammalian prion amyloids. *Cell*. 2005;121(1):63–72.
69. Vanik DL, Surewicz KA, Surewicz WK. Molecular basis of barriers for interspecies transmissibility of mammalian prions. *Mol Cell*. 2004;14(1):139–145.
70. Vorberg I, Groschup MH, Pfaff E, Priola SA. Multiple amino acid residues within the rabbit prion protein inhibit formation of its abnormal isoform. *J Virol*. 2003;77(3):2003–2009.
71. Kurt TD, Telling GT, Zabel MD, Hoover EA. Trans-species amplification of PrPCWD and correlation with rigid loop 170N. *Virology*. 2009;387(1):235–243.
72. Cutlip RC, et al. Intracerebral transmission of scrapie to cattle. *J Infect Dis*. 1994;169(4):814–820.
73. Cutlip RC, Miller JM, Lehmkuhl HD. Second passage of a US scrapie agent in cattle. *J Comp Pathol*. 1997;117(3):271–275.
74. Robinson MM, et al. Experimental infection of cattle with the agents of transmissible mink encephalopathy and scrapie. *J Comp Pathol*. 1995;113(3):241–251.
75. Fraser H, Bruce ME, Chree A, McConnell I, Wells GA. Transmission of bovine spongiform encephalopathy and scrapie to mice. *J Gen Virol*. 1992;73(pt 8):1891–1897.
76. Baron T, et al. Molecular analysis of the protease-resistant prion protein in scrapie and bovine spongiform encephalopathy transmitted to ovine transgenic and wild-type mice. *J Virol*. 2004;78(12):6243–6251.
77. Jeffrey M, et al. Oral inoculation of sheep with the agent of bovine spongiform encephalopathy (BSE). 1. Onset and distribution of disease-specific PrP accumulation in brain and viscera. *J Comp Pathol*. 2001;124(4):280–289.
78. Gonzalez L, et al. Phenotype of disease-associated PrP accumulation in the brain of bovine spongiform encephalopathy experimentally infected sheep. *J Gen Virol*. 2005;86(pt 3):827–838.
79. Martin S, Gonzalez L, Chong A, Houston FE, Hunter N, Jeffrey M. Immunohistochemical characteristics of disease-associated PrP are not altered by host genotype or route of inoculation following infection of sheep with bovine spongiform encephalopathy. *J Gen Virol*. 2005;86(pt 3):839–848.
80. Green R, Horrocks C, Wilkinson A, Hawkins SA, Ryder SJ. Primary isolation of the bovine spongiform encephalopathy agent in mice: agent definition based on a review of 150 transmissions. *J Comp Pathol*. 2005;132(2–3):117–131.
81. Robinson MM, et al. Experimental infection of mink with bovine spongiform encephalopathy. *J Gen Virol*. 1994;75(pt 9):2151–2155.
82. Wyatt JM, Pearson GR, Smerdon TN, Gruffydd Jones TJ, Wells GA, Wilesmith JW. Naturally occurring scrapie-like spongiform encephalopathy in five domestic cats *Vet Rec*. 1991;129(11):233–236.
83. Hamir AN, Kunkle RA, Cutlip RC, Miller JM, Williams ES, Richt JA. Transmission of chronic wasting disease of mule deer to Suffolk sheep following intracerebral inoculation. *J Vet Diagn Invest*. 2006;18(6):558–565.
84. Hamir AN, et al. Experimental transmission of chronic wasting disease agent from mule deer to cattle by the intracerebral route. *J Vet Diagn Invest*. 2005;17(3):276–281.
85. Raymond GJ, et al. Transmission and adaptation of chronic wasting disease to hamsters and transgenic mice: evidence for strains. *J Virol*. 2007;81(8):4305–4314.
86. Hamir AN, Miller JM, Kunkle RA, Hall SM, Richt JA. Susceptibility of cattle to first-passage intracerebral inoculation with chronic wasting disease agent from white-tailed deer. *Vet Pathol*. 2007;44(4):487–493.
87. Sawaya MR, et al. Atomic structures of amyloid cross-beta spines reveal varied steric zippers. *Nature*. 2007;447(7143):453–457.
88. Polymenidou M, Stoeck K, Glatzel M, Vey M, Bellon A, Aguzzi A. Coexistence of multiple PrPSc types in individuals with Creutzfeldt-Jakob disease. *Lancet Neurol*. 2005;4(12):805–814.
89. Wadsworth JDF, et al. Tissue distribution of protease resistant prion protein in variant CJD using a highly sensitive immuno-blotting assay. *Lancet*. 2001;358(9277):171–180.
90. Taraboulos A, Jendroska K, Serban D, Yang SL, DeArmond SJ, Prusiner SB. Regional mapping of prion proteins in brain. *Proc Natl Acad Sci U S A*. 1992;89(16):7620–7624.
91. Castilla J, Gonzalez-Romero D, Saa P, Morales R, De Castro J, Soto C. Crossing the species barrier by PrP(Sc) replication in vitro generates unique infectious prions. *Cell*. 2008;134(5):757–768.
92. Castilla J, Saa P, Hetz C, Soto C. In vitro generation of infectious scrapie prions. *Cell*. 2005;121(2):195–206.
93. Castilla J, Saa P, Morales R, Abid K, Maundrell K, Soto C. Protein misfolding cyclic amplification for diagnosis and prion propagation studies. *Methods Enzymol*. 2006;412:3–21.